Understanding the Scabbling of Concrete Using Microwave Energy

A.J Buttress[a]*, D.A. Jones*. C. Dodds*, G. Dimitakis*, C.J. Campell†, A. Dawson[b] , S. Kingman*,

*_ - Industrial Microwave Processing Research Group, Energy and Sustainability Research Division, The University of Nottingham, University Park, Nottingham, NG7 2RD, UK._

[b] _- Nottingham Transportation Engineering Centre, Infrastructure, Geomatics and Architecture research Division, The University of Nottingham, University Park, Nottingham, NG7 2RD, UK._

† - Sellafield Ltd Seascale, Cumbria UK.

[a] _- corresponding author adam.buttress @nottingham.ac.uk_

ABSTRACT: This paper reports on the use of microwave energy to scabble concrete. While the technique is not new, little information exists relating to the controllability of the process, the effect of different types of concrete and the performance and durability of the scabbled concrete post treatment. Concrete blocks supplied by the UK Sellafield nuclear site were treated with microwave energy using a 15kW system, operating at 2.45GHz. The effect of aggregate type (Whinstone, Gravel and Limestone); standoff distance; and effect of surface coating were studied to determine their influence on the systems performance, in terms of mass and area removal rates. Complimentary modelling studies were undertaken relating the power density of the microwave energy to observed scabbling profile. Mass and area removal rates averaged 11.3gs^{-1} and 3cms^{-1} respectively on treating large areas to a depth of 25mm. The process was shown to not adversely affect structural properties of the specimens after treatment.

KEYWORDS: Microwave Processing; Concrete; Radioactive Waste

1.0 Introduction

Scabbling is the mechanical process of removing a thin layer of concrete from a structure. For freshly laid concrete, the technique allows roughening of the surface, so paints can adhere to it. It also provides grip for wheeled machinery and reduces slip hazards for people and animals. During concrete rehabilitation, it can be used to remove imperfections or surface coatings [1]. As a tool for end-of-life processing, it can be used for the benefaction of Recycled Concrete Aggregate (RCA) by separating the relatively weak mortar from aggregate stone. Another application of concrete scabbling is to separate potentially harmful surface contaminated concrete which may contain heavy metals, organic substances (including PCBs) or radionuclides when concrete material is used in structures within nuclear facilities [2-4].

It is the latter application that is the subject of this paper. Over the last 40 years, 85 commercial power reactors, 45 experimental or prototype power reactors, as well as over 250 research reactors and a number of fuel cycle facilities have been retired from operation [5]. The vast majority of the radioactivity (approx. 99%) is contained within fuel that is removed on decommissioning. The

remainder is held in so-called 'activation products' like steel components that have been exposed to neutron irradiation over a long period of time and surface contamination of associated structures. Many of the concrete structures used in nuclear facilities have this residual radioactive contamination [2, 6, 7]. But often, the radionucleotide material is only contained in the concrete surface layer and typically comprises: strontium; caesium; cobalt; and uranium [8]. While this material is considered relatively low level waste, there is a need for an efficient system to remove the contaminated surface when decommissioning a site, so the remainder of the structure can be processed through a more conventional waste processing stream. By segregating the contaminated surface from the bulk concrete, reductions in the volume of radioactive material can be achieved leading to greater efficiencies in the downstream waste treatment process i.e. recycling; densification and disposal.

Mechanical methods for scabbling the surface layers of radionuclide contaminated concrete suffer from the problems associated with poor control over the depth of material removed [9]. The quality of the resulting surface can also be low leading to difficulty in additional remediation or processing. Excessive noise pollution and dust generation are also disadvantages [10]. Laser based techniques can also be used. Although the technique has been demonstrated at laboratory scale by a number of researchers [11-16], the development of a commercial system has not yet been achieved as it suffers from the perception that the capital costs are high and reliability is poor [17].

Microwave based treatment systems used for the end-of-life processing of cement and concrete have been shown at laboratory scale, to offer benefits over what could be considered traditional techniques [4, 18-20]. Microwave systems used to decontaminate concrete may reduce both the amount of radioactive material generated during the scabbling process, as well as airborne contaminants released into the environment. The technique also generates less noise than mechanical methods, and may be developed for remote operation, leading to a safer operator environment [9] and [21].

The actual mechanism by which the concrete is scabbled is still open to debate. The earliest work by White et al. [2, 22, 23] suggested that the rapid heating of pore water results in high steam pressures within the microstructure. This then causes explosive failure of the concrete in the heated zone. However, Bazant and Zi [24] reported an in depth mathematical treatment on the use of microwaves for this application. They concluded that the spalling action is the result of differential thermal stresses causing the surface concrete to explosively fail in compression when it is confined by cold concrete around the heated zone. While they acknowledged that pore pressure caused by the generation of steam does play a part, it was not considered to be a major contributing factor [24, 25]. They also showed that as the frequency of the incident wave increases from 0.896 to 18 GHz, the power dissipation is increasingly confined in the near surface. These results are in agreement with the work of Akbarnezhad and Ong [4]. Lagos et al. [7] also showed in their modelling studies that increasing the frequency confines the heating effect to the surface layers, leaving reinforcement bars deeper within the concrete largely unaffected. This is important for the development of an industrial system, since the objective is to separate the contaminated surface concrete leaving the bulk material structurally sound if it is to be remediated, or processed as an inert waste. Removal of the top surface

to a depth greater than were the contamination lies, not only creates excessive amounts of radioactive material, but may also damage the structure that is left behind.

While several patented concepts exist [22, 26, 27], there is relatively little experimental work has been reported. Much of the research was conducted between the late 1970s and early 1990s which still leaves opportunities for creating commercial scale systems. However, while the work reported to date has shown that microwave based scabbling is feasible, to develop a commercial scale system, fundamental understanding of how the process is controlled is required. This can then be used for the basis of design for an industrial system, which will then underpin the scale-up from laboratory studies to a pilot-scale unit.

This paper presents the results of material property testing undertaken to understand the fundamental interaction of the concrete with the applied energy and modelling studies to determine how the energy is dissipated within the material and compared to the results of the experimental trials. A number of issues key to the scale-up of the technique have also been addressed in this paper, including the influence of concrete composition on the scabbling process, an assessment of the controllability of the technique – specifically the effect of process conditions including residence time and stand-off distance, and also containment of ejected particulate matter.

Key objectives of the tests undertaken were to:

- determine the degree to which the removal (both depth and area) of material could be controlled by varying the microwave exposure time and the distance of the microwave applicator to the concrete surface (stand-off distance);
- determine the influence of concrete type on the performance (again as a function of depth and area removed) of the scabbling process; and
- understand how the generation of fines could be reduced during the scabbling process.

2.0 Experimental Methodology

2.1 Materials

Four concrete types were selected for this study and each was supplied by Sellafield Ltd. These were newly cured concrete samples which had been manufactured specifically for this study. They were cast from cement and three aggregate types: limestone, whinstone, and gravel, as these aggregates had been extensively used in the concrete structures at the Sellafield Nuclear site in the UK. Blocks of using each type of aggregate were cast having dimensions 1m x 1m x0.3m. The compositions of the concrete blocks used in the study are presented in Table 1.

Table 1: Composition of concrete blocks used the scabbling trials

	Proportion kg/m^3

Concrete Mix ID	Limestone	Gravel	Whinstone
OPC	330	330	330
Sand	680	650	700
4-10mm aggregate	400	380	460
10 – 20mm aggregate	830	830	930
w/c ratio	0.50	0.50	0.50
Slump (mm)	40-50	50-60	40

The Whinstone was obtained from Tarmac Ltd, Northern Area and supplied from Barrasford Quarry, Northumberland. The largely quartz sand was supplied by Armstrong's as standard concrete grade material and similar to that used at Sellafield. Cement was standard Ordinary Portland Cement (OPC), supplied from Castle cement.

2.2   Material Property Characterisation (TGA and Dielectrics)

The concrete specimens were characterised by determining their moisture content and dielectric properties. These are the key material characteristics that will govern their behaviour on application of the microwave energy [28-30]. Although conventionally TGA is used to identify chemical speciation due to loss of bound water and oxidisation with increasing temperature, here it was used to drive off the free water. This being defined as that held in the pore solution given that Almedia et al. [31], have shown that between 25 and 123.3°C, TGA causes the dehydration pore water in concrete. 9-11mg of each sample was heated at a rate of $2°min^{-1}$ up to 300°C under nitrogen ($300mlmin^{-1}$) using a Thermal Instruments Ltd. TGA Q500 SDT. The pore solution which is highly ionic, as a result it couples strongly to the applied microwave energy. So the greater the free water content of the concrete, the greater the heating effect and consequently the response to the scabbling treatment.

The dielectric properties were determined using the cavity perturbation technique. This technique has been used because of the relative simplicity of its design, and the ability to measure powdered samples at elevated temperature[32] [33] [29]. Dielectric properties are critical in all microwave systems to understand the response of the material to microwave energy and also to ensure efficient cavity/applicator design. In simple terms the dielectric properties consist of: the dielectric constant (ε'), which quantifies a materials ability to store electromagnetic energy through polarisation mechanisms, and the loss factor (ε'') which is a material's ability to convert this stored energy into heat through loss mechanisms [29].

A resonant circular copper cavity of diameter 550 mm and height 55 mm resonating in TM_{0n0} modes, was used for the measurement of dielectric properties [33] [34]. A measurement of the quality factor and resonant frequency using the empty tube is taken at a frequency of 912 MHz and 2.47 GHz. The

quality factor of a resonator (in this case the cylindrical cavity) is the ratio of the energy stored in the resonator to the energy dissipated in the dielectric material and the walls of the cavity per cycle. A representative powdered (<38µm) sample is then carefully weighed, and the height and diameter were then measured using a micrometer to determine its density. The sample holder was then reintroduced to the cavity, and the new resonant frequency and quality factor are measured. The dielectric constant and loss factor can then be calculated using perturbation equations [33]. The dielectric properties were then plotted as the value of the dielectric constant and loss factor as a function of frequency. Previous studies have shown that the determination of the dielectric constant and loss factor are accurate to 5 and 10% respectively using the cavity perturbation technique [32, 35]

2.3 Electromagnetic Modelling

The power density within the concrete block as well as the resulting heating response when subjected to microwave treatment was simulated numerically with the use of CONCERTO® 7.5 supplied by Vector Fields Ltd, UK. Figure 1 shows the simulated model. It consists of a waveguide and a concrete block with the background material set to air. No electrical conductivity value was specified for the waveguide section and was taken as perfect electric conductor. The concrete block was taken as dielectric and a *.pmo file containing the dielectric properties (as characterised in section 2.4.5), the enthalpy (J /cm^3) and the thermal conductivity (W/cm ^{o}C) with temperature was created. The values of the enthalpy were calculated by computing the integral of the specific heat capacity with temperature. The equations that calculate of the specific heat capacity and thermal conductivity with temperature for concrete containing siliceous were taken from Kodur and Sultan [36]. The density of the concrete block (2375 kg/m^3) was specified in the material properties. The TE$_{01}$ mode was excited in the waveguide, having polarisation normal to the broad face and the power and frequency of the source were taken as 15 kW and 2.45 GHz respectively. The dielectric properties of the air background were taken as □=1-j0. The boundaries of the concrete block were specified as adiabatic. Any further specification of boundary conditions is not required by the software as no plane wave was used.

Similar studies in the literature [24, 25, 37]have reported simulation results in a range of frequencies (2.45, 10.6, 18 GHz) however the present study focused exclusively on the use of 2.45 GHz. The choice of frequency was determined mainly by the availability of experimental equipment capable of generating the required level of microwave power (15 kW) at an ISM frequency. Out of the two ISM frequencies where equipment was readily available (0.896 MHz, 2.45 GHz) at the required power levels, the selection of 2.45 GHz deemed more appropriate as at this frequency water exhibits higher polarisation and thus providing an opportunity to study experimentally any effects associated with the heating of the water phase within the structure of concrete.

After the model is constructed and the parameters of the simulation are specified, a cubic mesh with the following details was created; Mesh cells: 3581424; Minimum cell sizes; X dimension: 3mm, Y dimension: 3mm, Z dimension: 3mm; Time-step: 0.00500346 ns. CONCERTO® uses a finite

difference time domain method (FDTD) [36] to compute the solution to the electromagnetic problem and then generates the resulting heating pattern by using the embedded basic heating module (BHM). The change in the dielectric and thermal properties of the concrete block with temperature are accounted for in the simulation via the *.pmo file. The total time covered by the simulation was 60 sec.
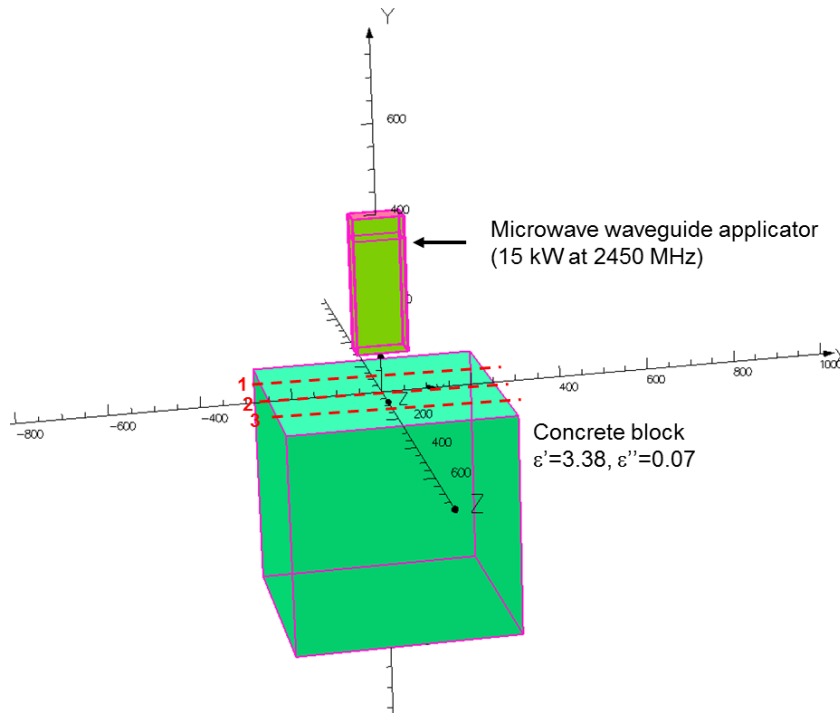

Figure 1: Illustration of Concerto[TM] model for electromagnetic simulation

When the simulation reached steady state the electric field distribution within the concrete block was calculated. The power density distribution within the volume of the concrete can also be computed. The electric field and power density inside a dielectric material are related by the following equation (Eq 1):

Equation 1 $$Power\ Density = 2\pi f \varepsilon_0 \varepsilon^2 E^2$$

Where: Power density W/m³, F = frequency (Hz), ε_0 = Permittivity of free space, ε"= Loss factor, E = electric field strength (F/m)

Once the power density distribution is computed the software calculates the temperature rise in the material for the time intervals specified by the user (5 sec in the present case), then the dielectric and thermal properties of the mesh cells are updated for the new temperature by the *.pmo file and the entire process thus far is repeated until the total time of the simulation is reached.

The effect of moisture content on the heating behaviour of the concrete block was not characterised separately. Instead direct measurements of the dielectric properties of the sample with temperature

were used in the model. Therefore, any effects due to changes in moisture level with temperature were accounted for indirectly by the changes that moisture level imparts on the dielectric properties of the material.

2.4 Microwave Scabbling Trials

The microwave concrete scabbling trials were undertaken using a Sairem microwave generator capable of delivering a variable power of up to 15kW operating at a frequency of 2.45 GHz. This frequency of operation was selected for a number of reasons; previous work had shown that microwaves at this frequency were effective in scabbling to surface to the necessary target depth [2, 6]; enables the terminating aperture to be of a suitable size relative to the trial blocks (section 2.1); and generators operating at this frequency are widely available. In addition, Microwave energy generated at a frequency of 2.45GHz has been shown in the literature - both in modelling studies and experimental trials, to scabble concrete successfully [2, 4, 6, 22, 25, 38].

The microwave power was delivered to the antenna through WR430 waveguide and an automatic E/H tuner manufactured by IBF electronics of Germany which was used for impedance matching purposes to minimise reflected power and thus maximise absorption of microwave energy.

Concrete breakage tests were performed within an electromagnetically screened room measuring 2.5 x 3.0 x 2.5 m. The concrete blocks measured 1 x 1 x 0.3 m with a grid of re-bar near the base for lifting purposes. The experimental setup is shown in Figure 2.
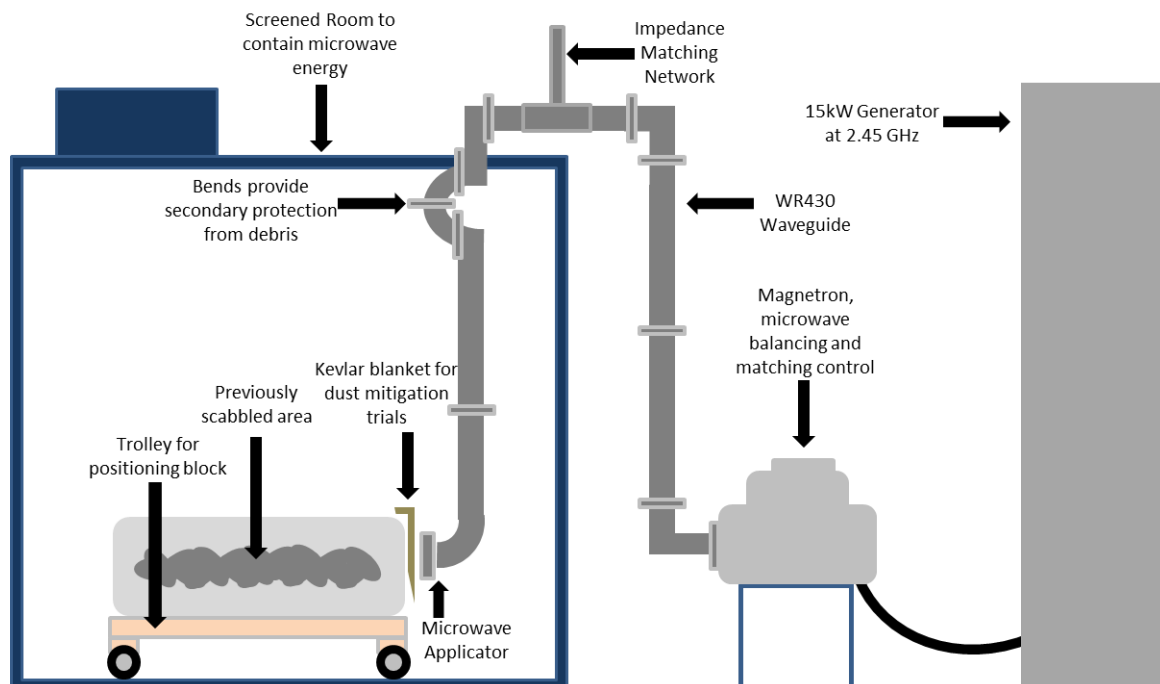

Figure 2: Experimental set up used for the scabbling trials

Within the room, a length of WR430 waveguide measuring 86 x 142 mm in cross section was selected for use as an antenna due to its robust structure, availability, and performance in previous sighter tests. The waveguide output was protected from debris by microwave transparent PTFE sheeting.

2.4.1 Post-treatment Characterisation – Brazilian Disc Strength Tests

Brazilian disc strength tests [39] were undertaken on samples recovered from the concrete blocks. This test was used to measure the indirect tensile strength. The aim of which was to quantify the strength loss post-treatment in the scabbled block to understand if the scabbling process damages the material underneath the scabbled area. A measured reduction in indirect tensile strength infers damage to the cementitious microstructure. This is an important consideration if the process is to be used for remediating existing structures and also to ensure the efficiency of the process is optimised to contain the scabbling effect in the topmost surface.

This technique was selected as it enabled the examination of the area closest to the scabbled surface. Previous studies performed at The University of Nottingham have used longer cores for Unconfined Compressive Strength (UCS) testing (not reported here) and these tests showed no change in properties between untreated and treated samples. This test method was chosen because the test specimens are relatively small and can be prepared from material recovered directly underneath the scabbled area. The sample arrangement for the Brazilian disc test is shown in Figure 3. Three samples were cored from each concrete block. One from an untreated area, a second through the surface of the scabbled area (Brazilian Specimen 1 termed 'upper') and third from underneath the upper disc (Brazilian Specimen 2, termed 'lower') as shown in Figure 3.
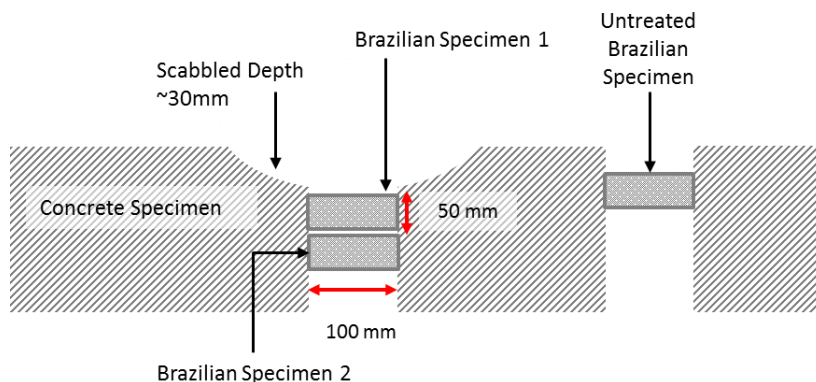

Figure 3: Sampling arrangement for Brazilian disc strength testing

2.4.2 Post-treatment characterisation – Scanning Electron Microscope (SEM) analysis

Following the microwave scabbling treatment, comparative analysis (untreated vs. treated) of concrete specimens was undertaken using a Scanning Electron Microscope (SEM). The SEM specimens were prepared from the Brazilian disc test samples. These were cut in half using a

diamond saw. A second slice was then taken though one half of the remaining cut specimens to enable an area of 25 × 25 mm to be imaged. This area was coated in Platinum using a sputter coater prior to introduction to the imaging chamber of the SEM. A FEI Quanta 600 in BSE mode, using a power of 25.0 kV and a spot size of 7.1 was used to capture images of the specimen's microstructure. The comparative SEM analysis of the specimens can identify damage to the cementitious microstructure. This could be manifested as microcracking through the cement-aggregate grain boundaries and/or possibly agglomeration of the void structure, either being as a result of the explosive release of steam pressure, or from the effect of differential thermal expansion during the scabbling treatment.

2.4.3 Post-treatment characterisation – Ultrasonic Pulse Velocity Tests

Ultrasonic Pulse Velocity (UPV) testing was also undertaken to characterise the damage to the concrete microstructure of the blocks as a result of the scabbling treatment. If microwave scabbling of the concrete has induced damage to the microstructure in the form of cracks and discontinuities (macrocracks), then the average transit time for the sound wave across a specimen will increase, resulting in a decrease in velocity. If a reduction in indirect tensile strength is not observed in the samples taken from the scabbled area, then it can be inferred that the scabbling effect is localised only in the material removed from the concrete block, thereby leaving the remaining surface free from damage. Further details can be found in [40].

The UPV test does not give information about the size and/or distribution of cracks, only that they exist. Indeed, the minimum measurable crack size for this frequency is unknown. The change in transit time may be used to evaluate the effect of microwave treatment; however, it is customary to convert transit time to UPV .

2.4.4 Thermogravimetric Analysis (TGA)

To ensure the relatively small mass of samples used in the TGA (9-11mg) was representative of the material, a 200g sample of the concrete was taken and gently ground in a mortar and pestle, then a micro-riffle was used to representatively sub-sample the material. Three samples were subject to TGA analysis and the average weight loss and derivative (% mass loss/°C) reported. Prior microwave trials have shown that only free water is evolved in the microwave breakage mechanism, as the temperature does not reach a sufficient level for the chemically bound water to be released (<200°C) [2] [38]. Above 120°C the rate of weight loss stabilises significantly to less than 0.01 % wt/min. In the absence of any further information from the supplier of the concrete blocks, the total weight loss below 110°C has therefore been taken to be representative of the free moisture content within the samples. The free moisture contents of the concrete samples as determined by TGA are shown in Table 2.

Table 2 : Free moisture content of the supplied concrete samples

Aggregate Type	Free Moisture Content (% wt. <110±0.5°C)
Limestone	2.26
Whinstone	2.15
Gravel	3.38

2.4.5 Dielectric property measurements

The results of the dielectric property measurements are shown in Table 3. Values for tap water and an aqueous salt solution are included for reference [29].

Table 3: Mean dielectric properties and free moisture content of concrete samples

Sample	912MHz		2470MHz	
	ε'	ε"	ε'	ε"
Limestone	2.86	0.09	2.85	0.08
Whinstone	3.19	0.16	3.33	0.08
Gravel	2.77	0.11	2.86	0.11
Tap Water	77	5.2	77	13
Salt Water (0.3M)	70	70	70	17

Note: ε' - dielectric constant, ε" – dielectric loss

Table 3 shows that there is little variation in dielectric properties of the concrete specimens cast using the different aggregates. From a dielectric point of view, concrete is a two phase mixture. The bulk of concrete consists of silicate and carbonate minerals, most of which are relatively microwave transparent and difficult to heat using microwave energy. The second phase which comprises a small percentage of the total is water, which is highly microwave absorbent as shown in Table 3. Water possess a high dielectric constant, showing a significant ability to be polarised by microwave energy. It also has a high dielectric loss factor because of the dissolved ions in the pore solution, so has the ability to convert this polarisation energy into heat very efficiently. Although the bulk dielectric properties of concrete are relatively low, it is the highly responsive water phase which absorbs the microwave energy. Considering Table 3, it would be expected that the value of the dielectric loss would increase when measured at 912MHz compared to 2470Mhz, as ionic loss mechanism's tend to dominate at lower frequencies [41]. However the measured values do not reflect this, with them being approximately the same at the two frequencies. This could be most probably attributed to the measured water contents being low, so the ability of the material to be polarised by whatever loss mechanisms predominate in the concrete is also low. However, as water is present in relatively small quantities and is the main absorbent phase, high power densities and therefore a rapid rate of heating on application of the microwave power can be achieved.

The dielectric properties of the Sellafield supplied concrete samples were measured at elevated temperature up to 250°C. This assists in understanding how the material will behave in an externally applied electromagnetic field throughout the process i.e. as temperature increases. The variation in dielectric constant and loss factor with temperature at 2.47 GHz is shown in Figure 4 and Figure 5 respectively.
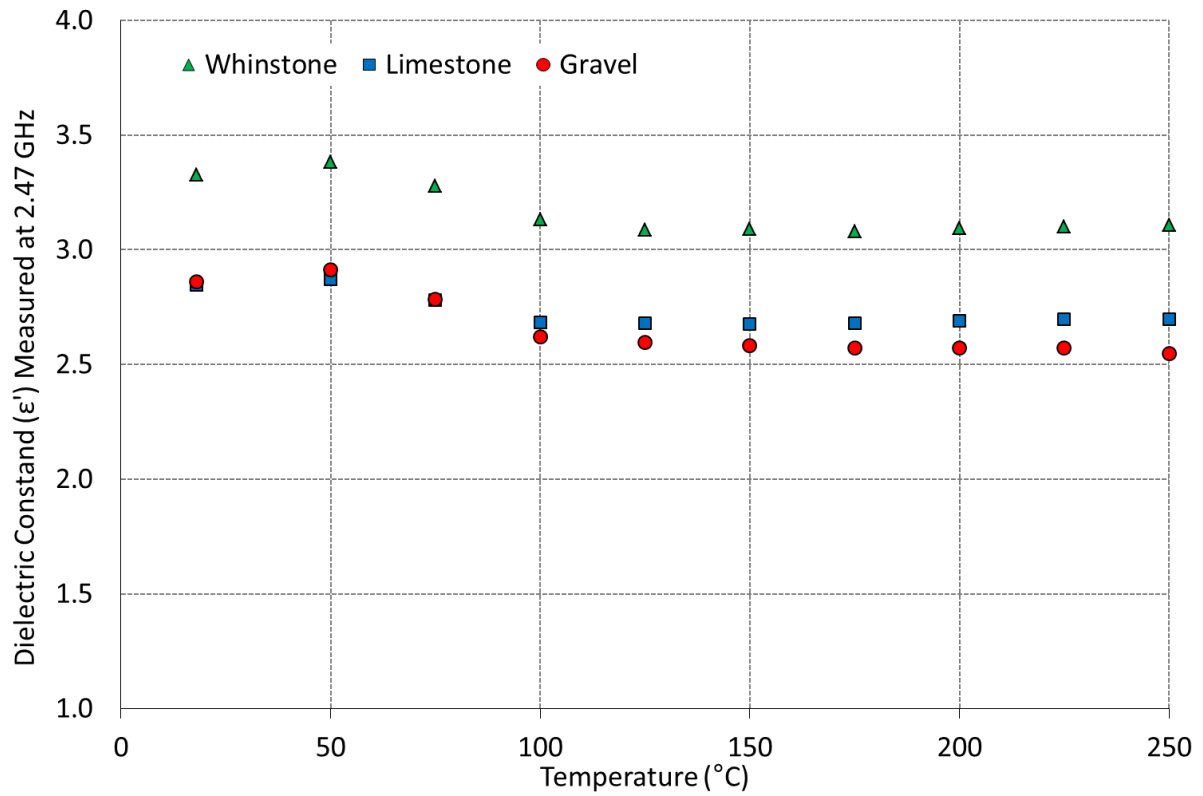
Figure 4: Relationship between the temperature and dielectric constant (ε') and temperature for the concrete samples measured at 2.47GHz by cavity perturbation technique
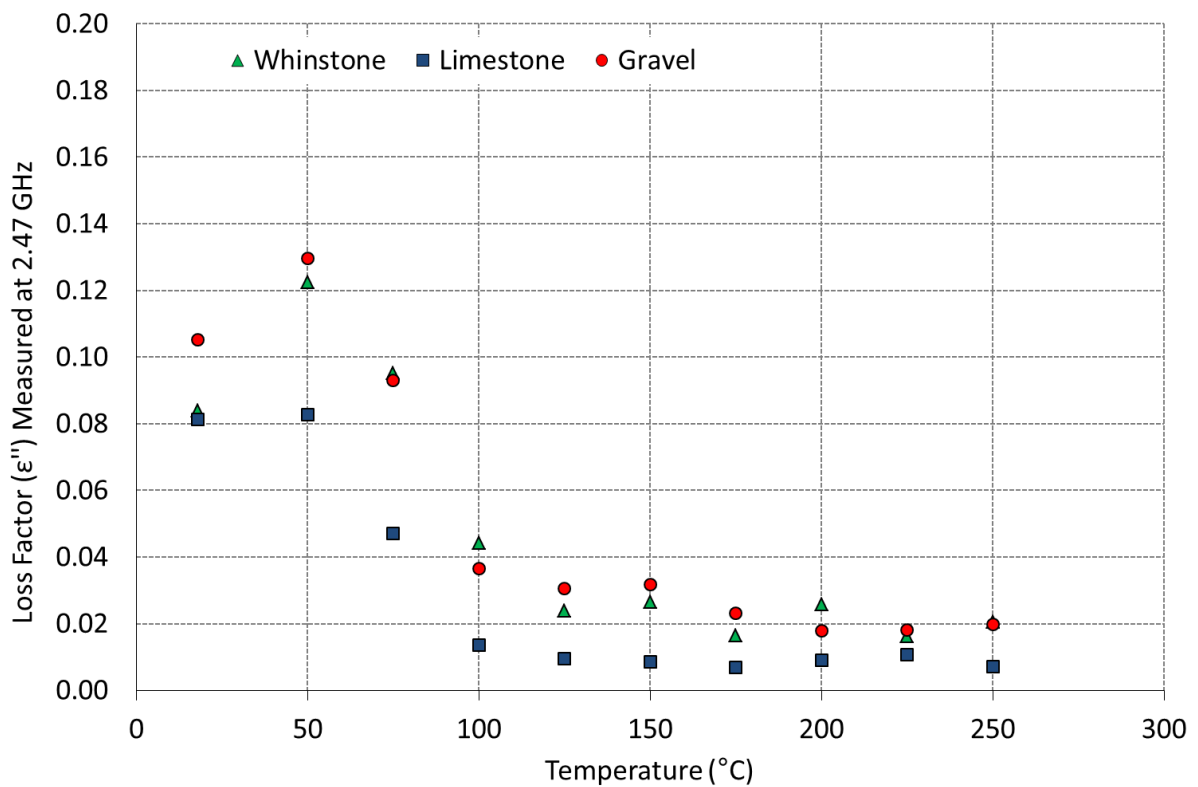

Figure 5: Relationship between the temperature and dielectric loss (ε") and temperature for the concrete samples measured at 2.47GHz by cavity perturbation technique

For all three concrete specimens, the dielectric constant and loss factor increase initially as free moisture is evolved from the cementitious matrix. This corresponds to an agglomeration of water droplets, coupled with the increased temperature, and resulting increase in ionic mobility. As water is lost and the ionic mobility reduces, the dielectric constant and loss also decrease. Then above 100°C, only the relatively microwave transparent concrete matrix remains, as the free water has been driven off. As suggested from the dielectric measurement data, above $100^{\circ}C$ the samples do not exhibit any substantial loss that could indicate susceptive behaviour upon exposure to microwave energy. Small variations in the loss at approximately $200^{\circ}C$ potentially are related to the presence of chemically bound OH groups. However, at this stage it remains unclear how these can influence the total heating behaviour of the samples. There are small variations in the dielectric properties of the concrete specimens, but these were not considered sufficient to influence the heating behaviour between the concrete specimens during the scabbling trails.

4. Electromagnetic Modelling Results

Figure 6 shows the power density distribution on the surface of the concrete block. The waveguide antenna is located above the concrete block and the microwave power is directly incident to the plane of the surface. Power density is defined as the power absorbed in the material per unit volume (W/m^3). Under microwave treatment, power density is proportional to the angular frequency of the microwave source, the absolute dielectric loss of the material and the second power of the electric field inside the material. The electromagnetic simulation software initially computes the electromagnetic field distribution within the material and uses the field values to produce the power density distribution.
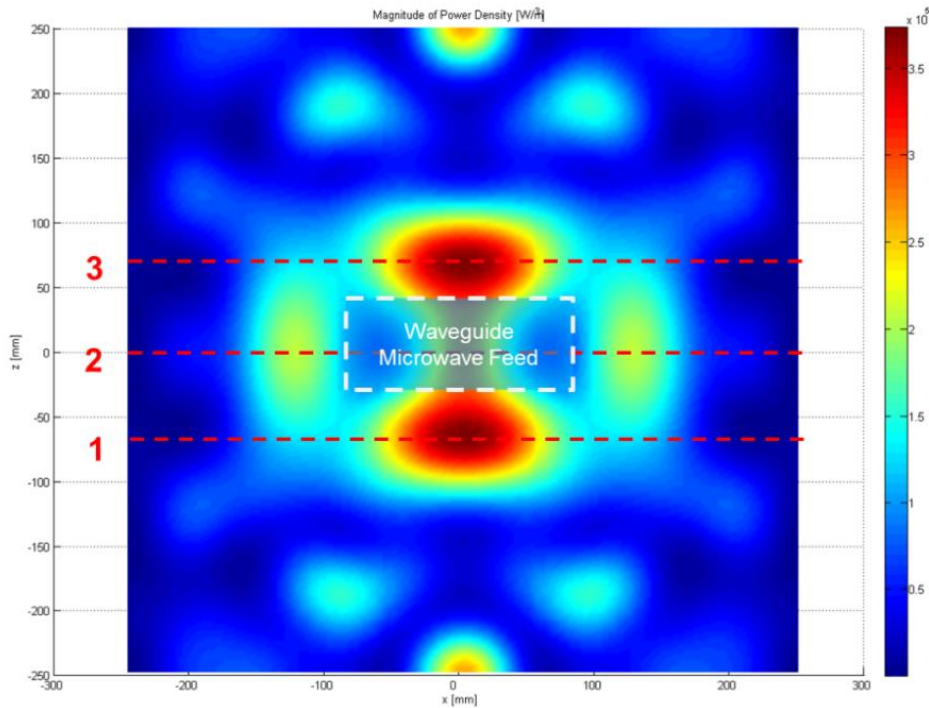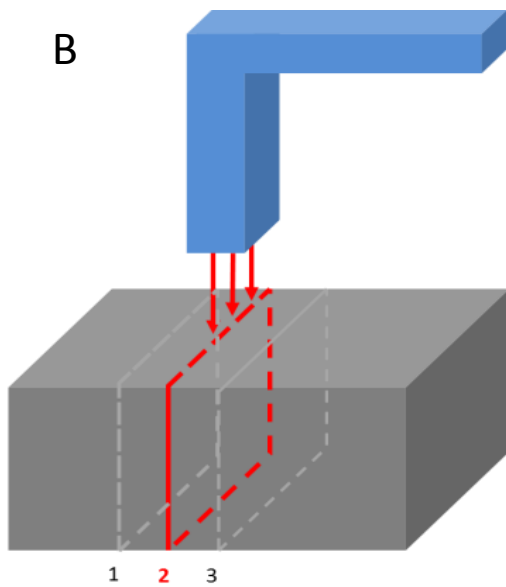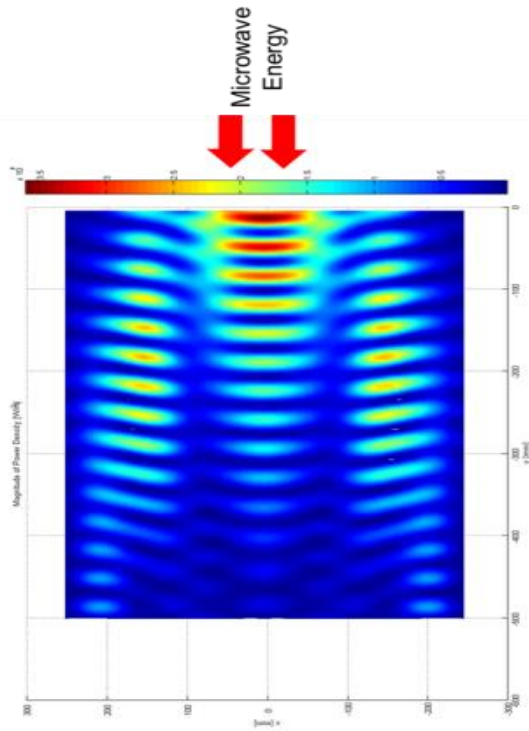
Figure 6: Simulation of the bulk power density produced in the surface of the concrete block directly underneath the waveguide. The microwave energy is incident to the plane of the surface.

The high power density distribution shown in Figure 6 corresponds to the lobes of the far field patterns of the waveguide antenna. Although a waveguide aperture is not an optimised antenna system, it is clear that it still possesses a substantial amount of directivity. To understand the variation in power density distribution with depth below the concrete surface, the simulation has been further investigated. Three slices into the block have been examined as shown by the dashed lines 1, 2 and 3. The power density distribution within these planes is shown in Figure 7 which also shows the shows the arrangement of the 2-D 'slices' though the concrete block used to calculated the power density distribution and the corresponding simulation results for that slice.
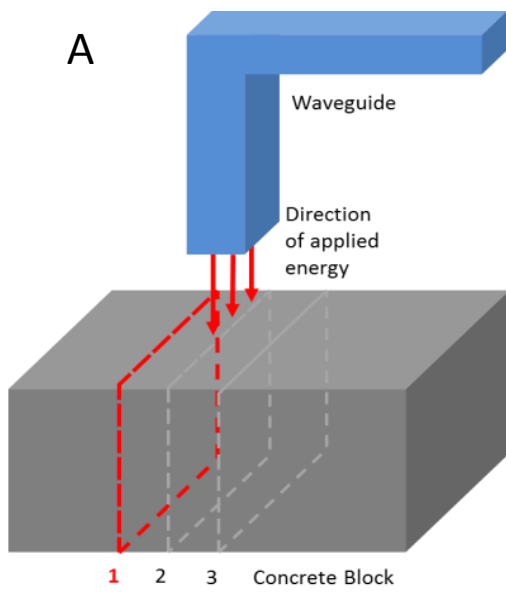
A

Waveguide

Direction
of applied
energy

Microwave
Energy

1   2   3   Concrete Block

2-D 'slices' through the block used in the
electromagnetic simulation

B

Microwave
Energy

1   2   3

2-D 'slices' through the block used in the
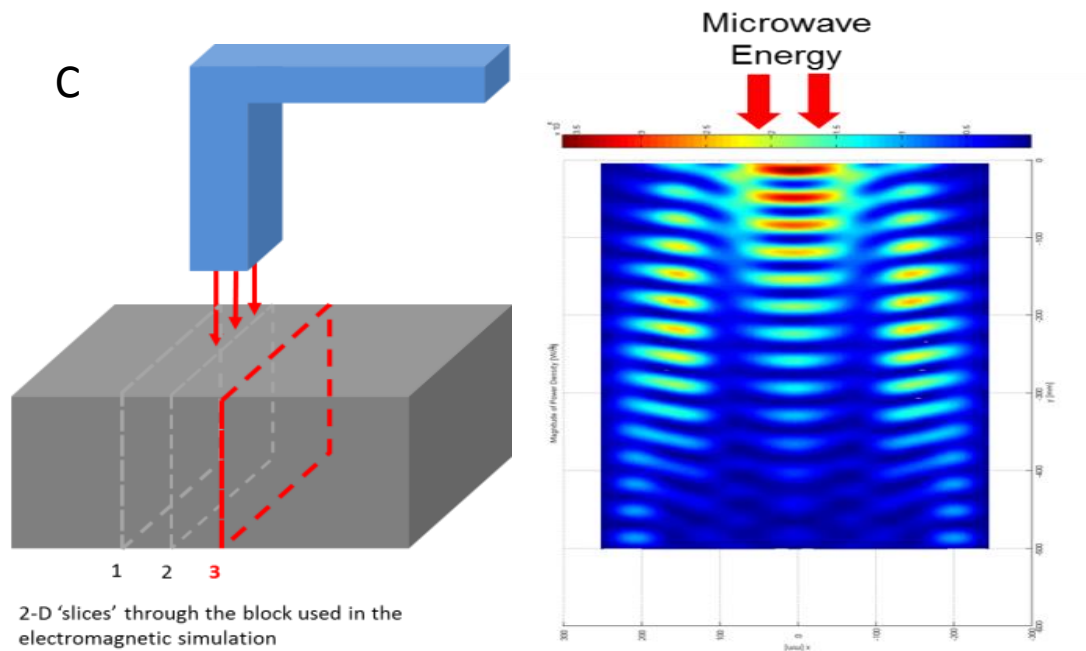electromagnetic simulation
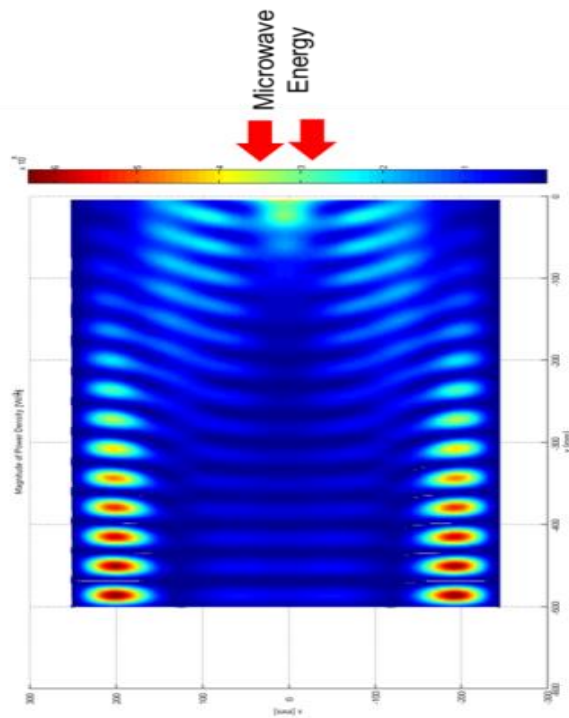
Figure 7: Arrangement of the three 2-D 'slices' (a – c) through the concrete block and the corresponding simulation results

The areas of high power density shown towards the rear of the block in Figure 7 are likely to be an artefact of the block dimensions used in the simulation, showing the reflection of the block-air boundary. If a block of larger dimensions were used in the simulation, it is expected that they would not be present. However, it can be concluded that microwave energy exhibits substantial penetration into the block and therefore high potential for interaction with microwave susceptible phases within the structure of concrete. Also a decrease in the wavelength of the propagating microwave energy, due to the dielectric constant of the concrete, can facilitate a fairly uniform treatment of the sample.

The power density distribution patterns presented in Figure 6 and Figure 7 and are identical and show a resonant pattern within the concrete block. The key output from these simulations was that the intensity of the power density decreases with increasing depth into the concrete. The two most intense areas of power density (shown by the red lobes) are situated at depths of approximately 0 – 20 mm and 40 – 60 mm. This is important as the areas of highest power density generated within the concrete block correspond to the areas where the scabbling mechanism will predominate. As described earlier, radionuclide contamination is generally contained in the top couple of centimetres. The maximum bulk power density shown in the simulations is approximately 3.5×10^5 W/m^3. These values are assume an applied microwave power of 15 kW, however they are directly scalable for changes in microwave power, so can be used to estimate power densities achieved within these samples at higher power levels.

Using thermodynamic properties from the literature [36], dielectric property measurements and the results from the simulation of the power density, the temperature evolved 6.5mm below the surface of the whinstone concrete was derived after 60s of treatment at 15kW and a standoff distance of 50mm. The result is shown in Figure 8a and 8b.
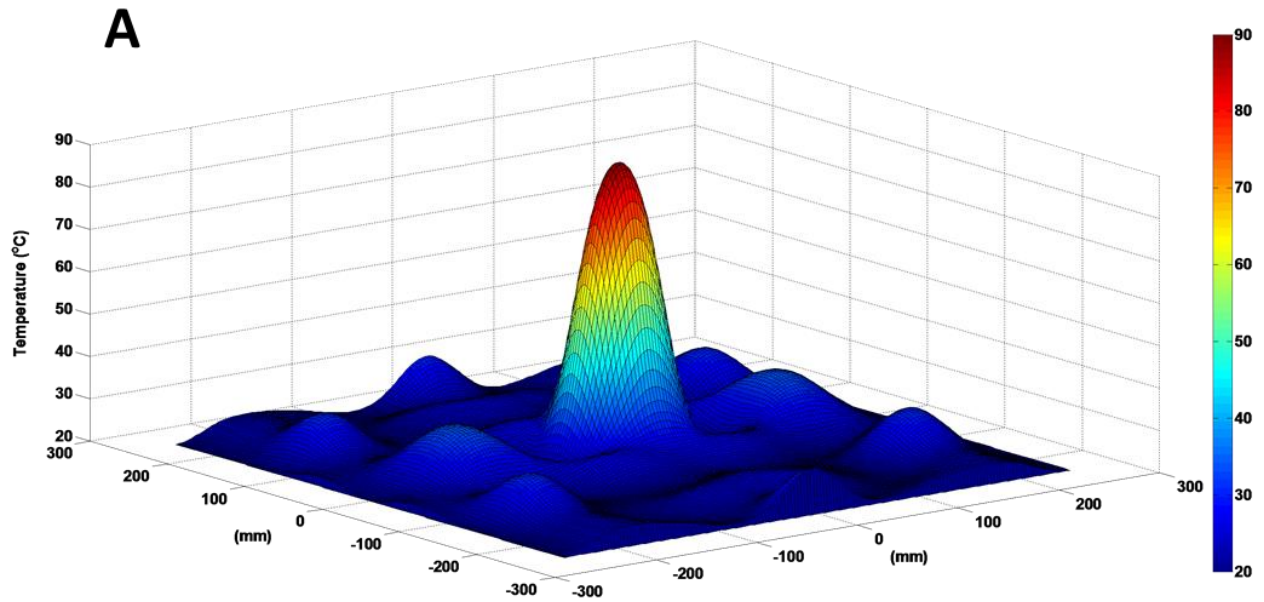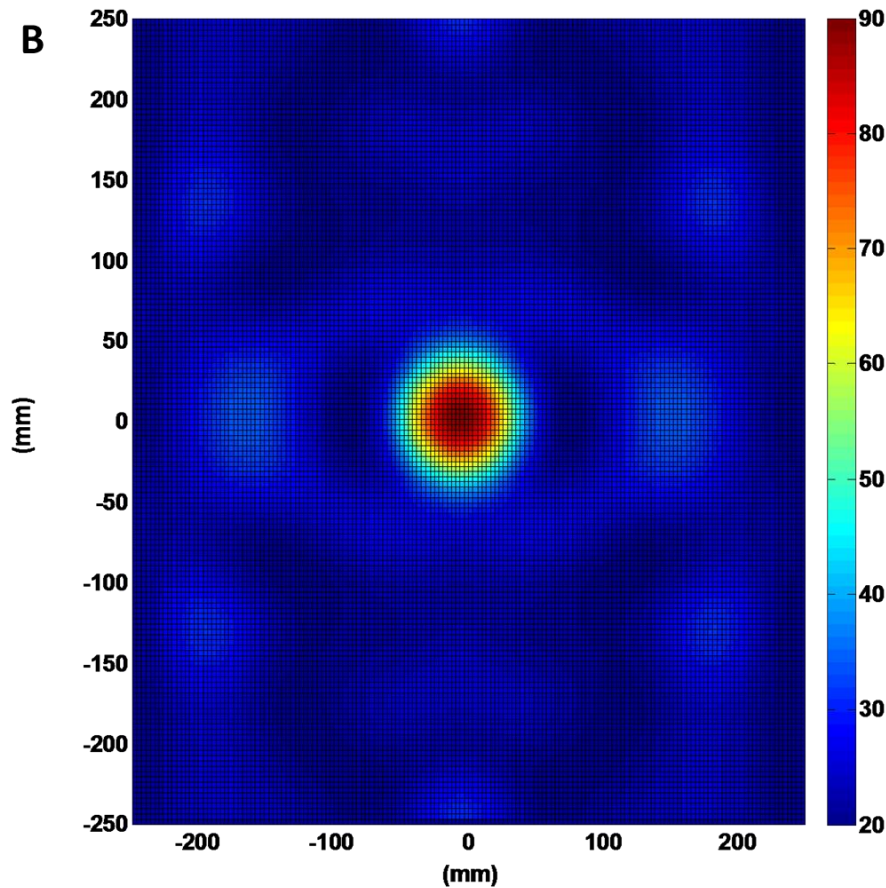
Figure 8: Evolved temperature 6.5mm below the surface of Whinstone concrete (15kW, 60s application time, 50mm stand-off distance)

It can be seen from Figure 8 that the concrete reaches a maximum temperature of 90°C. In reality the temperature within the pore solution of the microstructure will be much higher. This is a relatively simple model where dielectric properties of the bulk material have been used. Considering Table 3, the dielectric loss (ε") at 2.47GHz of bulk whinstone concrete is 0.08, compared to 13 for tap water, and 17 for a 0.3M sodium chloride solution. Pore solutions extracted from concrete having ionic strengths of 0.03 – 0.29M have been reported by [42]. Compared to the bulk concrete, the loss of the pore solution is orders of magnitude higher, so would be expected to be the dominant absorbent phase in the material. The temperature rise of the ionic solution within the pore structure would then be much higher than that derived from the modelling study shown in Figure 8.

The modelling studies undertaken by [37], showed that application of microwave energy at a frequency of 2.45GHz and power of 1.1MW/m^2 the concrete surface temperature increased from 25 to 80 $^{\circ}$C in only 5s. The power applied is close to that used in our studies (1.21 MW/m^2), however the dielectric properties used for the concrete had considerably higher values than the ones used in the present study and corresponded to saturated as opposed to air dry concrete. This can explain the longer time that took for the concrete to reach similar temperatures in the present study. Akarnezhad and Ong [37] showed that a temperature increase of 55 °C on the surface of the concrete yields a

radial compressive strength of 40 MPa in the near surface of the concrete. When the heated zone is confined by the cold concrete around it, this may well be sufficient to realise the physical scabbling effect.

In the present study a temperature increase of almost 70 °C has been calculated, inferring similar values of radial compressive strength may be generated in our samples, which could explain the scabbling observed experimentally.

Similar theoretical studies [24, 25, 37] dismissed the importance of the increased pressure of the steam generated by water trapped in the pores of the concrete (during microwave heating) as a plausible explanation for scabbling. Nevertheless,   whether the physical scabbling effect arises from steam pressure in the pores or differential thermal expansion of the solid phases, the modelling studies show that microwave treatment induces significant temperature rises (and as a result temperature differentials) in the near surface of the material.

5.0 Results and Discussion - Experimental Scabbling

5.1 Controllability of Technique and Influence of Concrete Type

Concrete is an inherently heterogeneous material. In order to investigate the controllability of the technique with respect to area and material removal rates, a matrix of experiments was performed scabbling large areas down the face of each block (ca. 1500cm^2). The blocks were exposed to 15 kW of microwave energy for one minute periods. Following each exposure, the test was paused and the block re-located within the screened room. All areas were scabbled to greater than the minimum target depth of 25mm and tests were repeated three times on each concrete type in order to gain some information on the variability of the technique. A depth of 25 mm was selected as an estimated value to remove all contaminated material based on the work of Spalding [8]. The tests required nine minutes of microwave exposure to produce a scabbled area of approximately 1 x 0.15m, as shown in Figure 10.
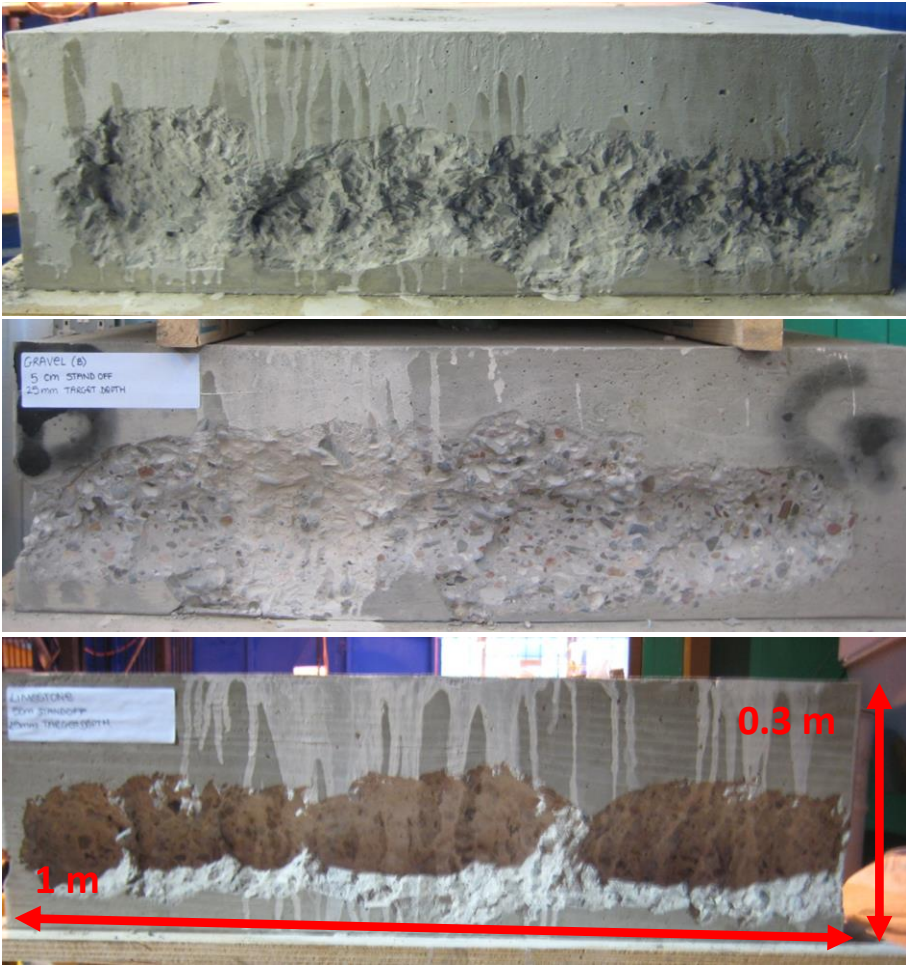
Figure 9: Scabbling results at 15kW, 60 seconds/location, 50 mm stand-off distance 25 mm target depth (Whinstone – top; Gravel – middle; and Limestone – bottom)

Figure 10 shows the variability in the total mass of concrete removed from a concrete block containing limestone, as a function of microwave exposure time. Mass ejected following 60 seconds of microwave exposure can vary from 500 to over 1100 g.
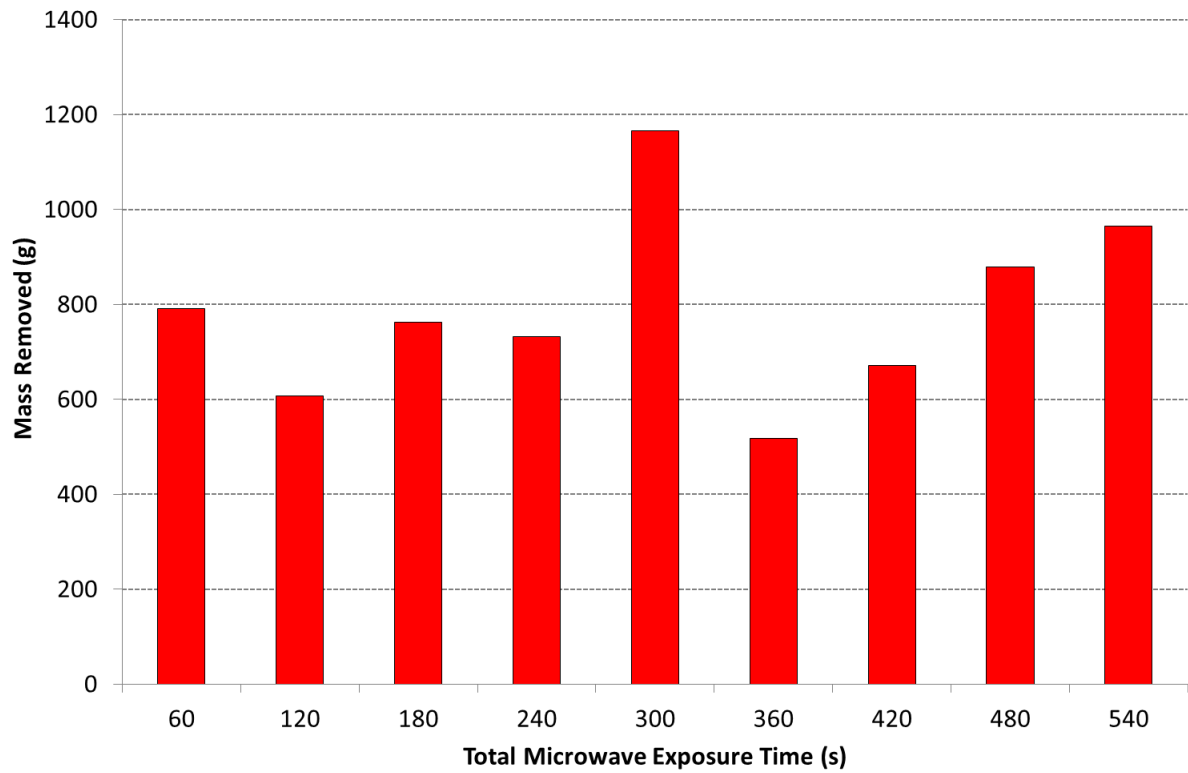
Figure 10: Variability in mass removal rates for each 60 second microwave exposure at 15 kW and 50 mm standoff distance for example limestone trial

The average material excavation rates for each nine minute treatment are shown in Figure 11.
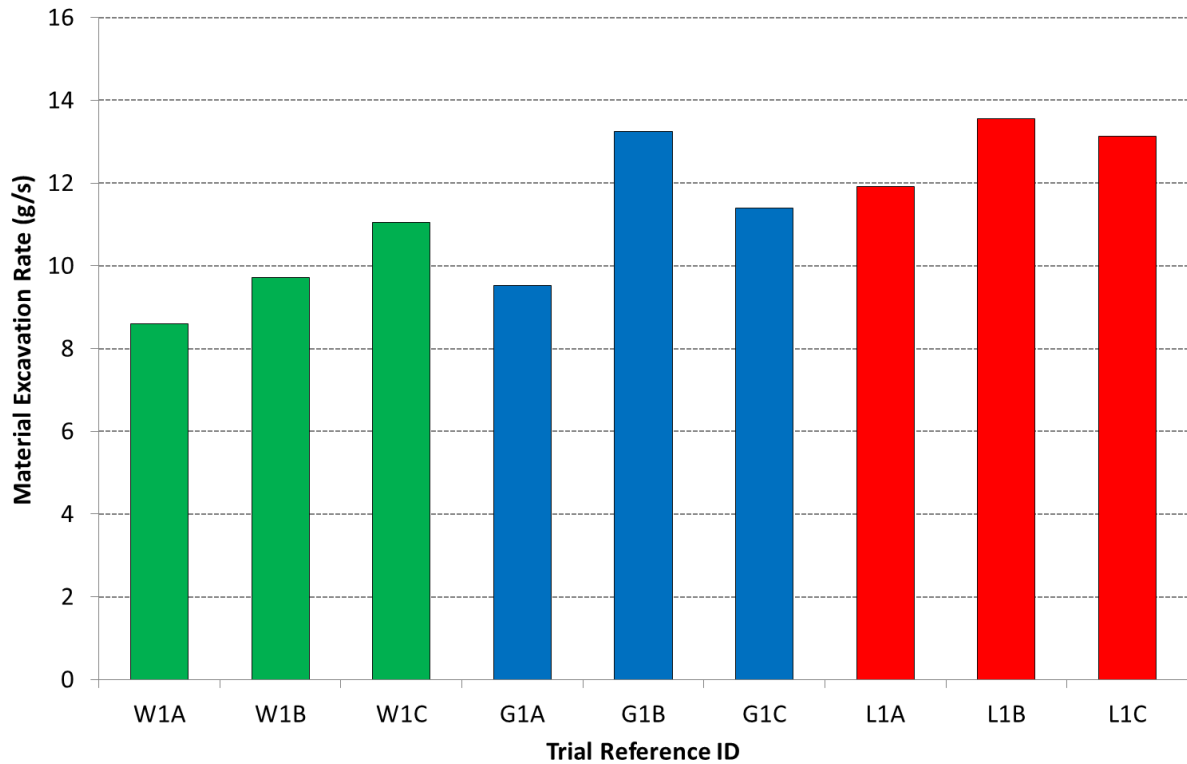
Figure 11: Average material excavation rates for each nine minute exposure and all concrete types on three specimens of each - a, b, and c. (applied power 15kW, standoff 50mm, W – whinstone concrete aggregate, G – Gravel concrete aggregate, L – Limestone concrete aggregate)

From Figure 11 it can be seen that all the concrete specimens tested can be successfully scabbled at mass removal rates of between 8.6 and 13.5g/s, irrespective of the type of aggregate used.

The standard deviations presented in Figure 12 show that there is a degree of variability in material removal rate for all concrete types. The greatest variability was observed in the gravel based aggregated based concretes (S.D. 1.86g/s) compared to S.D. 1.22g/s and 0.85g/s for Whinstone and Limestone concretes respectively. This may be partially due to a more rounded shape of the gravel aggregates, rather than the more angular shape of the Whinstone and Limestone, possibly resulting in weaker bonding forces within the structure. The total area scabbled was measured and mass removal rates above a minimum scabbled depth of 25mm equate to an approximate area removal rate of 2.0-2.8 cm^2/s.
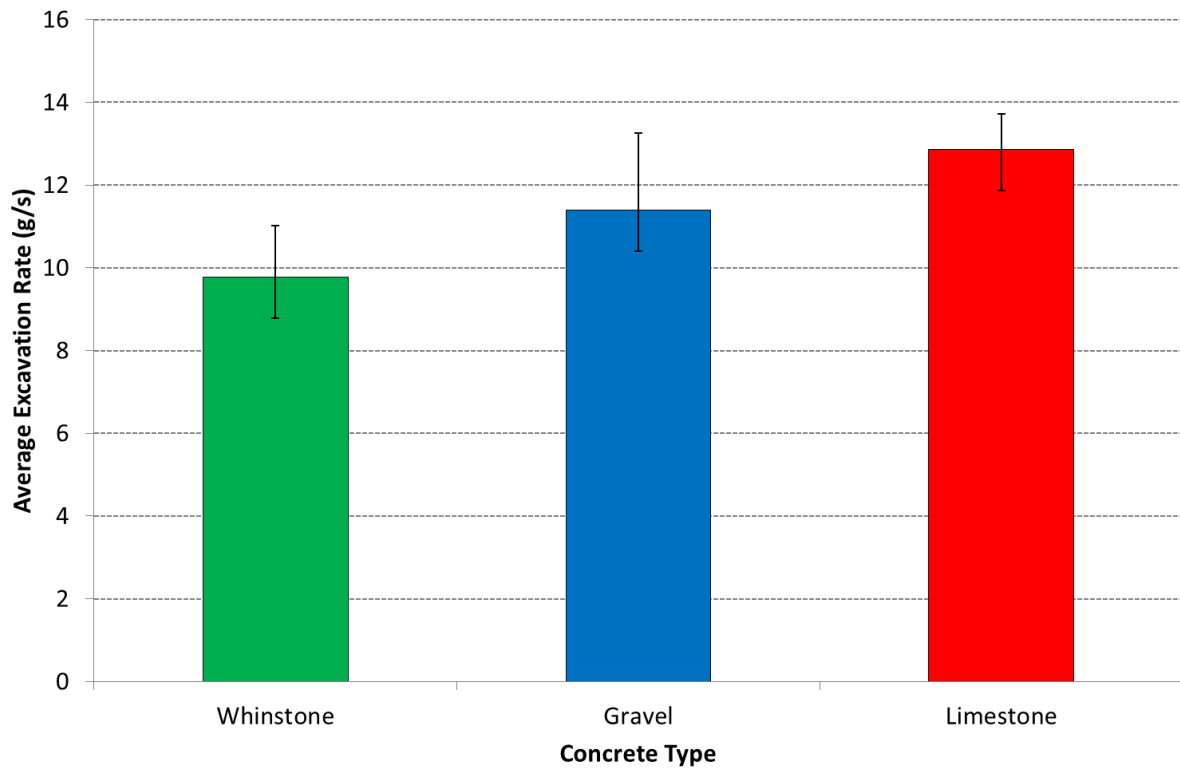
Figure 12: Mean overall material excavation rates and standard deviation for all concrete types (applied microwave power 15 kW standoff 50 mm)

It has been suggested that scabbling to a depth of greater than 5mm may be sufficient to facilitate man access into contaminated areas [23]. Figure 13 shows the change in mass removal rates when the required depth is reduced to 5 mm rather than 25 mm.
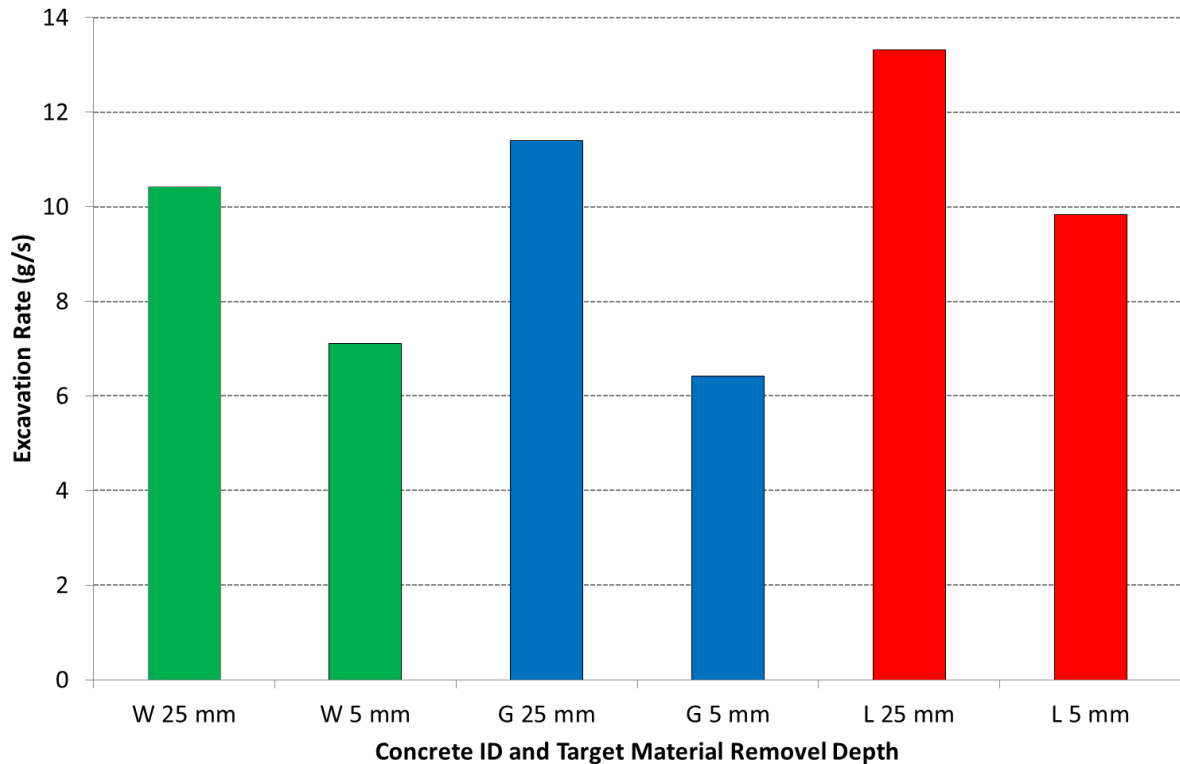
Figure 13: Influence of target removal depth on mass removal rates (applied microwave power 15 kW and 50 mm stand-off)

Figure 13 illustrates that the mass removal rate is reduced by 26-46% when the target depth is 5 mm compared to 25 mm. This is due to additional intervals required during the treatment to manoeuvre the block to a new position. These are twice as frequent comprising a 60 second break after every 30 seconds of treatment, rather than after 60 seconds of heating, as in the earlier study. However, as expected, the area removal rates increased slightly from 2.0-2.8 cm^2/s to 2.9-3.8 cm^2/s, as a result of the reduction in target depth. Given that the block must be moved manually, if the system could be automated as described in the introduction, then the process efficiency (in terms of mass removal and area treated) could be increased significantly.

5.2 Influence of Surface Coating and Standoff Distance

A further series of tests were performed to investigate if the mass or area removal rates could be enhanced by either coating the surface of the material with a solvent based paint or increasing the standoff distance from 50 to 100 mm. Figure 14 shows the influence of painting the surface and increased standoff on mass removal rates.
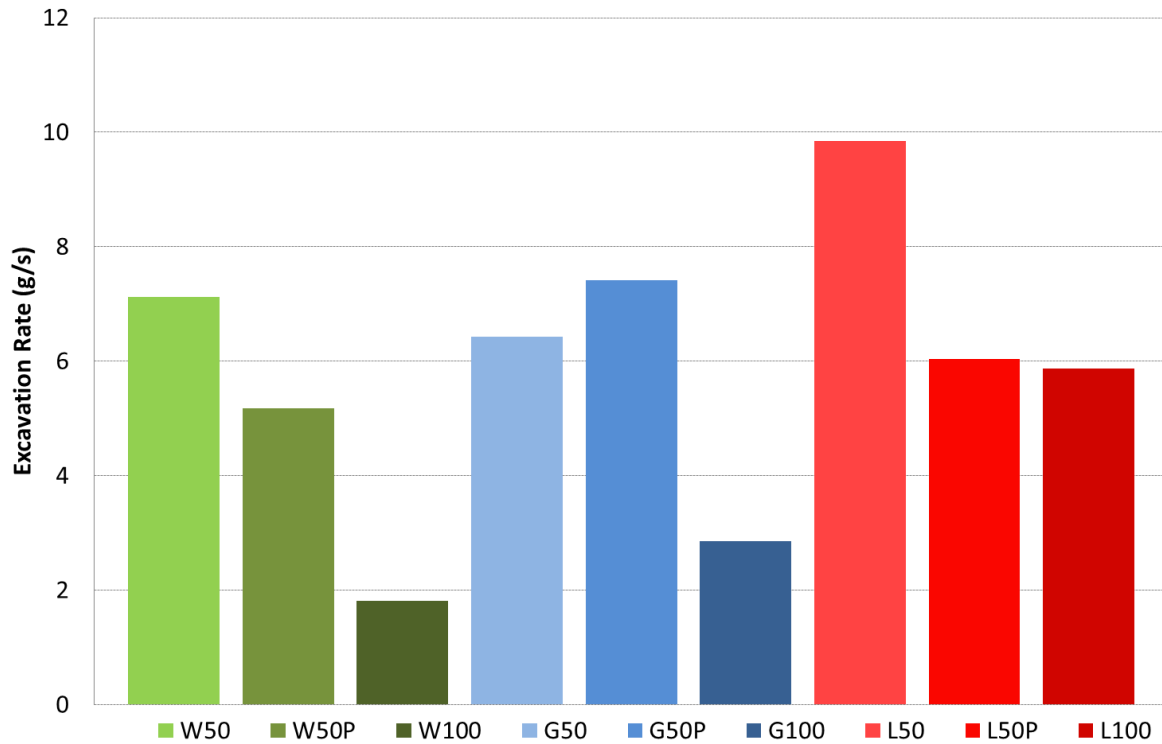
Figure 14: Influence of change in stand-off distance from 50 to 100 mm and painting the surface with solvent paints (P) on mass removal rates (applied microwave power 15 kW) Note: W – Whinestone, G – Gravel, L – Limestone, P – painted, 50 – 50mm, and 100 – 100mm

It can be seen from Figure 14 that an increase in standoff distance significantly decreases the excavation rate. The influence of painting the surface is inconsistent across the specimens tested and although some changes are evident, these are less than the statistical variability of the experiments. Exemplar results of these trials for the gravel-based concrete specimens are shown in Figure 15..

Figure 15: Effect of stand-off distance and painting the gravel-based concrete surface post treatment at 15kW (50mm stand-off – top, 100mm standoff – middle, painted surface 50 mm stand off – bottom)

Further work would be required to accurately quantify any potential effect. Rock wool, glass/Kevlar blanket and lexan™ bullet proof screen were also considered as surface coatings. Rock wool and glass/Kevlar blanket were very effective at mitigating dust and debris and lexan™ would be suitable for use as a blast screen to protect the microwave hardware, but none of these materials appeared to have any significant influence on material removal rates. Increasing the power of the system and moving to a lower frequency would improve system performance and efficiency. The optimisation of antenna design, standoff distance and potential surface coatings would also factor in the future development of an industrial system. This is considered more fully in section 6.

5.3 Particle Size Distribution (PSD) of Scabbled Material from Limestone Concrete (15kW, 50mm Standoff Distance for 1 Minute)

Particle size distribution analysis was performed in order to investigate the generation of fine particulates when scabbling with microwave energy to enable comparison with other technologies. An analysis was performed on a limestone based concrete sample which had been subjected to one minute's exposure at 15 kW applied microwave power and 50 mm standoff distance. These

conditions were selected as they were used for the bulk of the controllability studies. The PSD was determined through dry screening using woven wire sieves according to the British Standard BS1796 [43]. Figure 16 shows the cumulative particle size distribution for the excavated material.
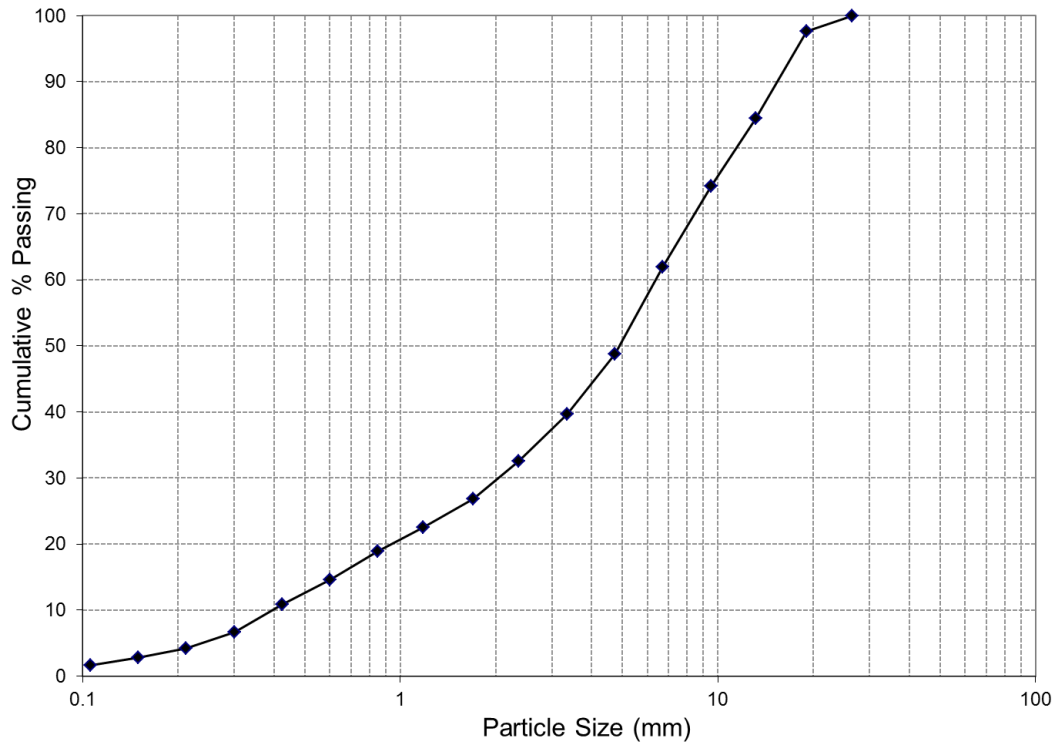

Figure 16: Cumulative particle size distribution of microwave scabbled material from limestone sample (1min exposure, 15kW applied power, 50mm standoff)

The surface coatings such as rock wool and kevlar / glass blanket considered in Section 5.2 have been shown to significantly reduce airborne particulates. The particle size distribution of the scabbled material shown in Figure 16 shows that the total quantity of small particulates is relatively low with only 1.6% of the total material ejected passing 106 μm and 80% larger than 1 mm. The use of a CO_2 laser for concrete scabbing was reported by [44]. They found that less than 1% of the liberated material was sub 100 μm which compares well with these results. In comparison in a microwave scabbling trial reported by [2] less than 1% of the debris produced by during their scabbling trials was smaller than 1mm. So material liberated was coarser than that reported in these trials. It is suggested that the PSD of the scabbled material using microwave processes is more a function of concrete composition rather than the parameters of the microwave treatment.

5.5 Strength Testing

A 100mm core was diamond drilled from beneath a scabbled area produced from a single 1 minute exposure (15kW applied power and 50mm standoff distance). Another identical core was removed from an untreated area of block. A 100 × 50 mm disk was extracted from each core for Brazilian disk testing to determine its unconfined compressive strength. A schematic of the areas from which the Brazilian samples have been taken is shown in Figure 3. The peak failure load and linear displacement is shown in Table 4. The change in peak failure load and total absorbed energy before failure are shown in Table 4.

Table 4: Results of the Brazilian disc tests for the concrete specimens treated at 15kW, 50mm standoff distance for 60s

Disc ID	Whinstone		Limestone		Gravel	
	Failure Load (kN)	Displacement (mm)	Failure Load (kN)	Displacement (mm)	Failure Load (kN)	Displacement (mm)
Untreated	25.5	0.66	29.4	0.70	23.3	0.73
Upper	18.5	0.59	24.8	0.60	16.6	0.60
Lower	22.6	0.80	33.7	0.74	21.2	0.66

Table 5: Change in Brazilian disc tensile strength of cores taken from treated blocks expressed as a percentage of the untreated controls

| Sample	Change in Peak Failure Load (%)	Change in Total Energy Absorbed Before Failure (%)
Whinstone Upper	-28.3	- 34.3
Whinstone Lower	-8.39	-21.6
Limestone Upper	-15.5	-23.6
Limestone Lower	+14.6	+8.2
Gravel Upper	-30.0	-15.7
Gravel Lower	-11.7	+28.7

The results show a 16-34% reduction in total energy absorbed before failure in the region immediately beneath the scabbled area. Further Brazilian disc tests were performed on the treated lower discs shown in Figure 3 in order to quantify the depth of material which has been affected by microwave scabbling. These second samples showed variation from 22% reduction to a 29% increase in total energy absorbed before failure. This indicates that any change in post-treatment material properties

are less than inherent variability of the concrete material itself and the measurement techniques. This is indicative of a highly heterogeneous material. A similar relationship exists when examining peak failure load with the upper Brazilian Specimen showing 16-30% reduction and then -12-+15% variability in the lower Brazilian Specimen.

There is a strong correlation between the predicted power density distribution and two lobes of high power density (shown previously in Figure 6), with the region from which the samples were taken (shown in Figure 3). The first is likely to represent the area where the surface material has been scabbled and the second the area beneath which has shown some reduction in strength. The results shown suggest that the affected area is relatively concentrated in the near-surface, as shown by the electromagnetic simulations, and by previous studies which considered bulk properties over a greater depth into the material.

5.6 Scanning Electron Microscopy (SEM)

Results of the SEM analysis of the treated and untreated concrete samples are shown in Figure 17. As can be seen from the micrographs, there is no discernible difference in the microstructure of the concrete samples analysed. No evidence of micro-cracking was observed in the majority of the areas subject to the SEM analysis.
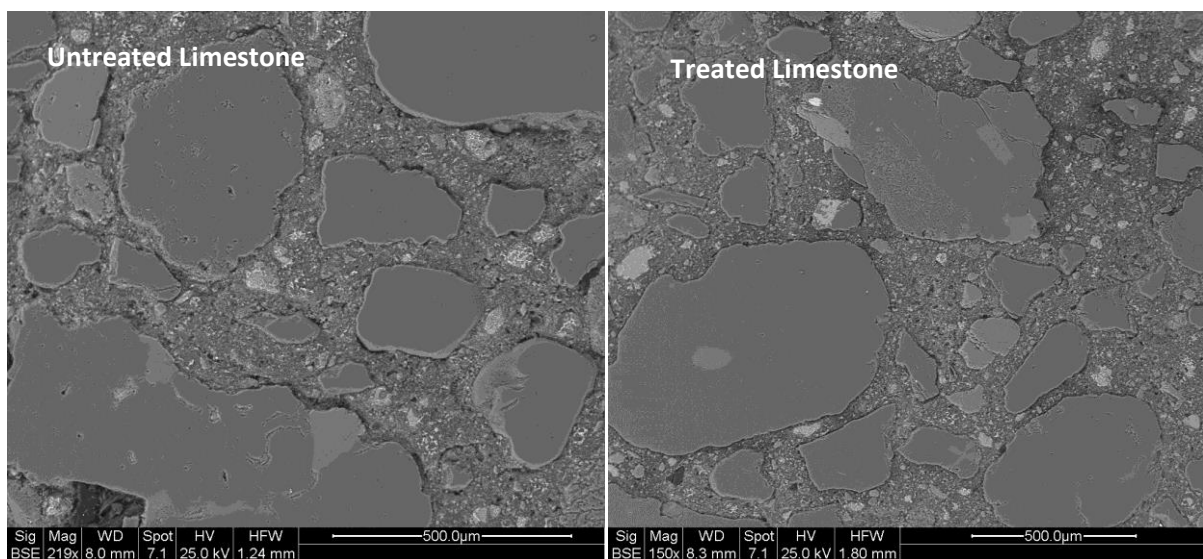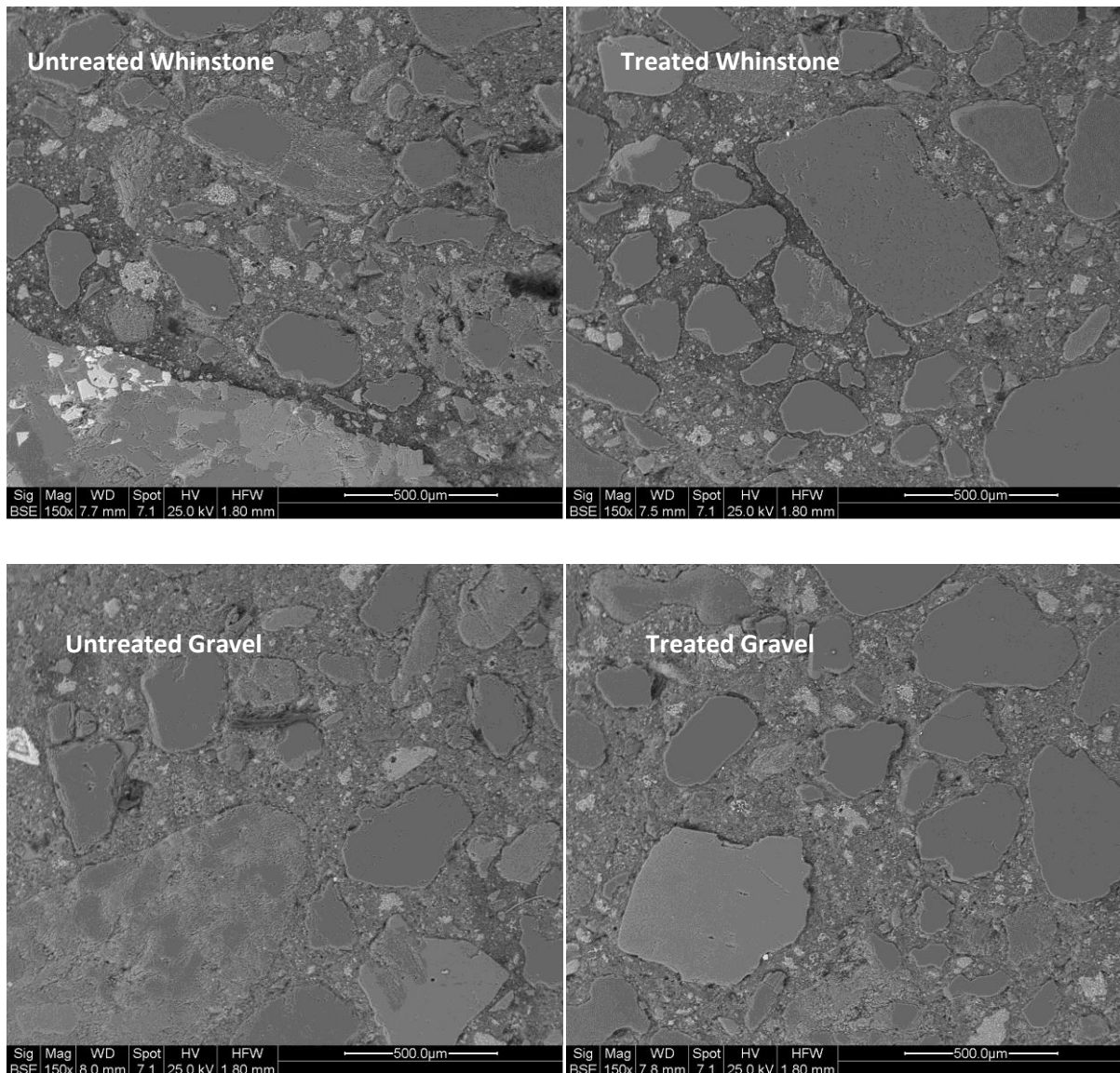
Figure 17: SEM images of untreated vs. treated concrete samples

After extended study of the SEM samples, microstructural damage of some discrete areas of the treated Whinstone and Gravel concrete samples were observed. These are highlighted in red and shown in Figure 18. The damage to the microstructure may have arisen as either be a result of microwave scabbling, and would support the results of the Brazilian disc tests, showing some reduction in strength, or could potentially be caused by the fracture which takes place during the Brazilian disc test itself.
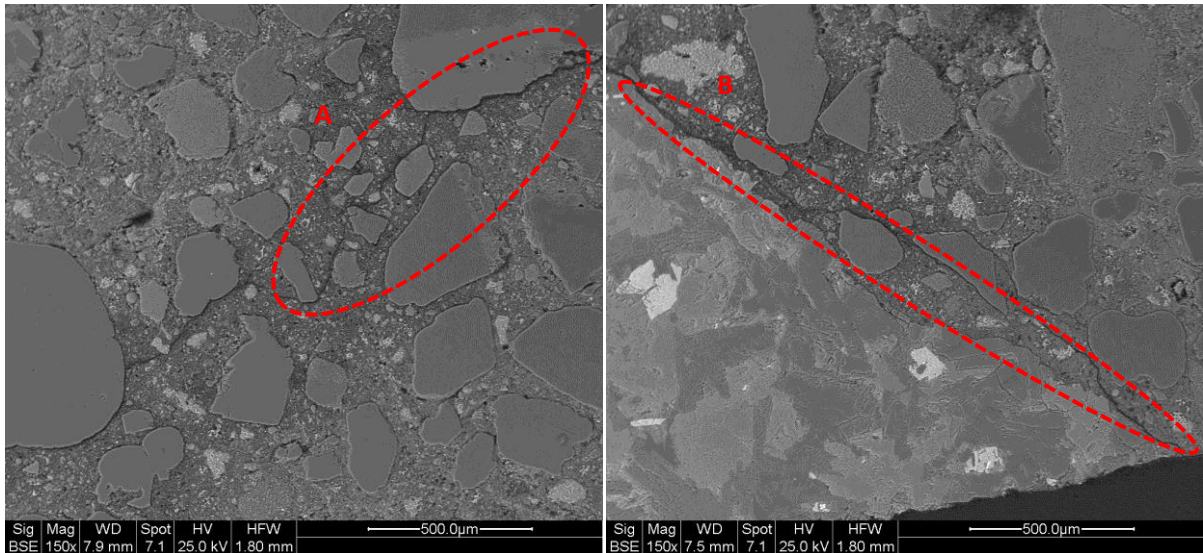
Figure 18: SEM images of micro-fractures in the treated Whinstone (left, A) and Gravel (right, B) based concretes

5.7 Ultrasonic Pulse Velocity (UPV) Tests

The UPV tests were undertaken using the method described in section 2.4.3. Six measurements were taken on each of the treated and untreated Brazilian disc samples and the average value was recorded. The results of the UPV measurements showed a reduction in UPV of 4.2, 1.4, and 3.6% for limestone, gravel and whinstone respectively. Although this may suggest some small degree of cracking, the standard deviation of the measurements was 2.8 – 7.3% and in each case greater than the recorded change. Although no reliable conclusions can be drawn from the UPV tests this presents a useful technique worthy of further investigation.

One possible future application would be to measure UPV across a large block at varying depth beneath the area which it is intended to be scabbled. By repeating the measurements following microwave scabbling this may provide useful data on any damage and the depth to which it protrudes.

6.0 Discussion

All of the concrete blocks used in the microwave scabbling trials were scabbled successfully. There were relatively small variations in removal rates between concretes made with the three different aggregate types, with the most material being removed from the limestone based concrete (12.9g/s) and the least from the Whinstone (9.8 g/s). From an electromagnetic perspective, the three concrete types are largely the same, as their measured dielectric properties are similar. This implies that their interaction with the applied energy and thereby heating rates would also be comparable. So it is

probably just general variability in the process, rather than the specific composition of the concrete affecting the scabbling process. This is supported by the fact that there was no discernible difference in the response to microwave treatment of the aged concrete sample compared to the other concrete blocks. This indicates that the technique could be relatively versatile in terms of the range of concretes that could be treated.

The results of modelling the power density distribution through a concrete block and the evolved temperature in the material on treatment showed that power density and corresponding heating effect is confined to the near surface, which correlated well with the observed physical scabbling results. Temperature measurements were not taken of the blocks either during or after treatment, but should additional work be undertaken, this would provide useful information as to which physical mechanism underpins the scabbling effect; either pore pressure or differential thermal stresses in the solid phase. The effect of concrete with differing water contents and how this changes the interaction with the applied microwave energy could also be studied. While a number of in-depth modelling studies have been undertaken [7, 24, 25, 38], these have not been validated against experimental trials. However, defining this was not one of the objectives of the study, but is certainly a recommendation for further work.

By varying the standoff distance it was shown that the closer the waveguide aperture is to the surface, the more material is removed. In practice, the open waveguide would need screening and protecting from the released debris and would be a necessary part of the ruggedisation of the technology.

In all the materials, concrete was removed to a depth greater than 25mm. This is generally deeper than where the radionuclide contamination is held. This suggests that the process could be further optimised to target a shallower depth and increase the area removal rates. In the present trial, these were significantly affected by having to manually relocate the block after each treatment. Automation of the process to allow for continuous surface treatment with minimum operator input, which would facilitate significantly higher treatment rates.

Importantly, performance testing of samples taken from the concrete blocks showed that their strength was not significantly affected by the microwave process, indicating that the microstructure of the concrete directly beneath the removed area is not damaged. This was supported by the results of the SEM analysis which found very little evidence of material fracture within the cementitious microstructure of the samples taken from the concrete blocks post treatment. These results show that a microwave based scabbling technique could be used to rehabilitate existing structures, without affecting their long-term performance and durability.

The containment of airborne particulate matter would be critical to the safety of a commercial system. The results showed that the PSD of the scabbled material was comparable to that derived from laser based scabbling with very little being <100 µm, the size fraction which is generally considered airborne. It was found that the containment of particulates was relatively straightforward and could be

achieved by covering the treatment area with a microwave transparent fabric such as Rock Wool or Kevlar.

To increase the efficiency of the system, the frequency of the applied energy could be reduced to the next ISM band of 896MHz, as this increases the size of the waveguide aperture. Significant engineering challenges would still have to be faced with respect to controllability of the system, portability, and ruggedisation such that it is practical to use in the field.

In the immediate term, further work is recommended to understand the response of a wider variety of concrete materials to the scabbling process to confirm the versatility of the technique. Additional performance characterisation of the materials, post-treatment, should be undertaken to further investigate the effect the scabbling process has on the performance and durability of the remaining concrete, both on the surface and at depth. Trials should be conducted using a system based on microwave energy at a frequency of 896MHz, to understand how system efficiencies could be improved.

7.0 Conclusions and Recommendations for Further Work

During the course of this work, over 20, 000cm^2 of concrete has been scabbled successfully. Under all test conditions, the microwave scabbling equipment used was able to successfully treat all the specimens irrespective of process conditions. This included the use of repeated exposures and the treatment of corners and edges of the specimens.

For a scabbling event to occur in a given specimen, it will be dependent on the action of a number of variables to a lesser or greater degree dependant on which mechanism predominates:

- Moisture content of the specimen - this will affect the dielectric properties and consequently the interaction of the material with the applied energy. The pore solution is ionic so is expected to be the principal absorbent phase in the material.
- Power density within the cement matrix - this will have a direct effect on the rate of temperature rise of the pore solution and thus internal pressures generated for any given concrete; in addition to affecting the c stresses arising from the interface of heated material and the cold surrounding concrete confining it.
- The permeability of the material - this will have a significant impact on any internal pressures generated (and their subsequent dissipation). If the concrete is excessively permeable, then elevated pressures generated via liberation of vapour-phase moisture will be more easily dissipated, thereby preventing the pressure exceeding the strength of the concrete; and
- Tensile strength - affects the ability of a concrete surface to be scabbled using microwave energy as this affects the stresses arising from differential thermal expansion. All the modern and stiffest concrete specimens, as treated during this study responded very favourably to scabbling treatment.

Brazilian disc strength testing showed that the tensile strength of the area immediately beneath the scabbled surface was affected up to a depth of 50mm. However, SEM analysis showed no signs of micro-cracking beneath the scabbled area that could unambiguously be attributed to the microwave treatment.

Mass removal rates have averaged 11.3 g/s when treating large areas to greater than 25 mm depth and area removal rates approximately 3 cm^2/s. In these trials the microwave treatment was paused at least every 60 seconds to relocate the block to a new treatment area. This allows the steam pressures created to dissipate and therefore area and mass removal rates are likely to significantly increase with continuous microwave exposure in an industrial system.

The use of rock wool and glass / Kevlar blanket have been shown to significantly reduce the generation of dust and airborne particulates however particle size analysis showed that only 1.6% of the excavated material was smaller than 106µm in diameter.

The rate of removal (mass and area) will be a function of both power level and frequency. It is highly likely that significantly higher removal rates would be possible at the next ISM allocated frequency of 896 MHz, which has a wavelength which is 2.7 times longer (approximately 33 cm rather than 12 cm). It is calculated (based on frequency scaling) that area removal rate would increase to approximately 22 cm^2/sec and mass removal rate would increase to approximately 81 g/s. These increases are also still assuming intermittent microwave exposure and would be in addition to any benefits realised from continuous treatment.

The mechanism by which the physical scabbling effect arises should be investigated. Whether it is by pore pressure or differential thermal expansion, by defining the mechanism and carrying out trials on a wider range of concrete materials, the versatility of the technique and its application to industry can be assessed.

References

[1] A. Echt, W. Sieber, A. Jones, E. Jones, Control of Silica Exposure in Construction: Scabbling Concrete, Applied Occupational and Environmental Hygiene, 17 (2002) 809-813.

[2] T.L.G. White, R.G. Pugh, L.P., Foster, D. Box, W.D., Removal of contaminated concrete surfaces by microwave heating – phase 1 results, Proceeding of the International Symposium on Waste ManagementTucson AZ USA, 1993, pp. 745 - 748.

[3] H. Klee, Recycling Concrete, in: S. Development (Ed.) Cement Sustainability InitiativeWashington D.C., 2009.

[4] A. Akbarnezhad, K.C.G. Ong, M.H. Zhang, C.T. Tam, T.W.J. Foo, Microwave-assisted beneficiation of recycled concrete aggregates, Construction and Building Materials, 25 (2011) 3469-3479.

[5] W.N. Association, http://www.world-nuclear.org/Information-Library/, 2013.

[6] T.L. White, D. Foster Jr, C.T. Wilson, C.R. Schaich, Phase 2 microwave concrete decontamination results, Oak Ridge National Lab., TN (United States), 1995.

[7] L. Lagos, W. Li, M. Ebadian, T. White, R. Grubb, D. Foster, Heat transfer within a concrete slab with a finite microwave heating source, International journal of heat and mass transfer, 38 (1995) 887-897.

[8] B.P. Spalding, Volatility and Extractability of Strontium-85, Cesium-134, Cobalt-57, and Uranium after Heating Hardened Portland Cement Paste, Environmental Science & Technology, 34 (2000) 5051-5058.

[9] C.H. Oh, Hazardous and Radioactive Waste Treatment Technologies Handbook (Handbook Series for Mechanical Engineering), 1 edition ed., CRC Press; 1 edition (14 May 2012)2001.

[10] M. OBrien, R. Meservey, M. Little, J. Ferguson, M. Gilmore, Idaho National Engineering Laboratory Waste Area Groups 1-7 and 10 Technology Logic Diagram. Volume 2, EG and G Idaho, Inc., Idaho Falls, ID (United States), 1993.

[11] L. Johnson, R. Rogers, M. Hamilton, L. Nelson, J. Benson, M. Green, Biodecontamination of Concrete Surfaces: Occupational & Environmental benefits, Lockheed Idaho Technologies Co., Idaho Falls, ID (United States), 1996.

[12] M. Savina, Z. Xu, Y. Wang, M. Pellin, K. Leong, Pulsed laser ablation of cement and concrete, Journal of Laser Applications, 11 (1999) 284.

[13] M. Savina, Z. Xu, Y. Wang, C. Reed, M. Pellin, Efficiency of concrete removal with a pulsed Nd: YAG laser, Journal of Laser Applications, 12 (2000) 200.

[14] S. Wignarajah, New horizons for high power lasers: applications in civil engineering, Proceedings of SPIE in High-Power Lasers in Civil Engineering and Architecture, 3887 (2000) 34-44.

[15] P.L. Crouse, L. Li, J.T. Spencer, Laser-Based Cutting of Contaminated Concrete, ASME, 2003.

[16] V. Kumar, R. Goel, R. Chawla, M. Silambarasan, R.K. Sharma, Chemical, biological, radiological, and nuclear decontamination: Recent trends and future perspective, Journal of Pharmacy And Bioallied Sciences, 2 (2010) 220.

[17] P. Hilton, C. Walters, The potential of high power lasers in nuclear decommissioning, Paper at WM 2010 Conference, Phoenix, AZ, 2010, pp. 7-11.

[18] W. Alexander, Methods of cracking structures and apparatus for cracking structures, Google Patents, 1969.

[19] H. Yasunaka, M. Shibamoto, T. Sukagawa, Microwave decontaminator for concrete surface decontamination in JPDR, Proceedings of the Int. Decommissioning Symposium, 1987, pp. 109-115.

[20] N. Lippiatt, F. Bourgeois, Investigation of microwave-assisted concrete recycling using single-particle testing, Minerals Engineering, 31 (2012) 71-81.

[21] T.L. White, D.J. Foster, C.T. Wilson, C.R. Schaich, Phase 2 microwave concrete decontamination results, Oak Ridge National Laboratory, Oak Ridge, TN USA, 1995.

[22] T.L. White, T.S. Bigelow, C.R. Schaich, D. Foster, Mobile system for microwave removal of concrete surfaces, Google Patents, 1997.

[23] T.L. White, D.J. Foster, C.T. Wilson, C.R. Schaich, Phase 2 microwave concrete decontamination results, Oak Ridge National Laboratory, Oak Ridge, TN USA, 1995.

[24] Z.P. Bazant, G. Zi, Decontamination of radionuclides from concrete by microwave heating. I: theory, Journal of engineering mechanics, 129 (2003) 777-784.

[25] G. Zi, Z.P. Bazant, Decontamination of radionuclides from concrete by microwave heating. II: Computations, Journal of engineering mechanics, 129 (2003) 785-792.

[26] B.F. Casagrande, J.P., Microwave applicator and method for the surface scarification of contaminated concrete, 1998.

[27] J.P. Furtlehner, A. Hugla, Focusing microwave applicator, 2000.

[28] L. Dongxu, W. Xuequan, A study on the application of vacuum microwave composite dewatering technnique in concrete engineering, Cement and Concrete Research, 24 (1994) 159-164.

[29] R.J. Meredith, Engineers' handbook of industrial microwave heating, IET1998.

[30] N. Makul, P. Keangin, P. Rattanadecho, B. Chatveera, D.K. Agrawal, Microwave-assisted heating of cementitious materials: Relative dielectric properties, mechanical property, and experimental and numerical heat transfer characteristics, International Communications in Heat and Mass Transfer, 37 (2010) 1096-1105.

[31] A.E.F.d.S. Almeida, E.P. Sichieri, Thermogravimetric analyses and mineralogical study of polymer modified mortar with silica fume, Materials research, 9 (2006) 321-326.

[32] R.G. Hutchison, J.T. Chang, H.M. Jennings, M.E. Brodwin, Thermal acceleration of Portland cement mortars with microwave energy, Cement and Concrete Research, 21 (1991) 795-799.

[33] M. Arai, J. Binner, G. Carr, T. Cross, High temperature dielectric property measurements of engineering ceramics, Ceram. Trans., 36 (1993) 483-492.

[34] N.R. Greenacre, Measurement of the high temperature dielectric properties of ceramics at microwave frequencies, University of Nottingham, 1996.

[35] C.J. Dodds, Microwave treatment of carbonaceous materials, University of Nottingham, 2006.

[36] V. Kodur, M. Sultan, Effect of temperature on thermal properties of high-strength concrete, Journal of materials in civil engineering, 15 (2003) 101-107.

[37] A. Akbarnezhad, K. Ong, Microwave decontamination of concrete, Magazine of Concrete Research, 62 (2010) 879-885.

[38] K. Ong, A. Akbarnezhad, Thermal stresses in microwave heating of concrete, Proc. 31st Our World in Concrete and Structures, (2006) 297-310.

[39] Z. Bieniawski, M. Bernede, Suggested methods for determining the uniaxial compressive strength and deformability of rock materials: Part 1. Suggested method for determining deformability of rock materials in uniaxial compression, International Journal of Rock Mechanics and Mining Sciences & Geomechanics Abstracts, Elsevier, 1979, pp. 138-140.

[40] J.H. Bungey, M.G. Grantham, S. Millard, Testing of concrete in structures, Crc Press2006.

[41] W. McCarter, P. Curran, The electrical response characteristics of setting cement paste, Magazine of Concrete research, 36 (1984) 42-49.

[42] K. Andersson, B. Allard, M. Bengtsson, B. Magnusson, Chemical composition of cement pore solutions, Cement and Concrete Research, 19 (1989) 327-332.

[43] BSI, Test sieving. Methods using test sieves of woven wire cloth and perforated metal plate, BS 1796-1, 1989.

[44] L. Lobo, K. Williams, E. Johnson, J. Spencer, Particle size analysis of material removed during CO_2 laser scabbling of concrete for filtration design, Journal of Laser Applications, 14 (2002) 17-23.